Hindawi Publishing Corporation
Conference Papers in Energy
Volume 2013, Article ID 395659, 7 pages
http://dx.doi.org/10.1155/2013/395659

Conference Paper

Caustics as an Alternate of Ray Tracing to Evaluate Heliostat Mirrors

Marios D. Georgiou,[1] Aristides M. Bonanos,[2] and John G. Georgiadis[1,3]

[1] *Department of Mechanical Science and Engineering, University of Illinois at Urbana-Champaign, Urbana, IL 61801, USA*
[2] *Energy Environment and Water Research Center, The Cyprus Institute, 2121 Nicosia, Cyprus*
[3] *The Cyprus Institute, 2121 Nicosia, Cyprus*

Correspondence should be addressed to Aristides M. Bonanos; bonanos@cyi.ac.cy

Received 3 December 2012; Accepted 4 February 2013

Academic Editors: Y. Al-Assaf, P. Demokritou, A. Poullikkas, and C. Sourkounis

This Conference Paper is based on a presentation given by Aristides M. Bonanos at "Power Options for the Eastern Mediterranean Region" held from 19 November 2012 to 21 November 2012 in Limassol, Cyprus.

Solar thermal power generation is based on the concept of concentrating solar radiation to provide high temperature heat for electricity generation via conventional power cycles. The high relative cost of optical subsystems necessitates a careful study of their components. The capital cost of the heliostat field in central receiver power plants is significant, reaching up to 50% of the capital investment. Therefore, it is essential to maximize the energy yield from a heliostat with a given mirror area. Solar collector fields are typically modeled by ray-tracing or convolution methods; however, no general method is available for engineering analysis. We propose the use of caustics to predict the image of the sun reflected by an arbitrary mirror of focal length F and aperture a on a target. The method of caustics was validated against SolTRACE, a ray-tracing code developed by the US National Renewable Energy Laboratory (NREL).

1. Introduction

The global energy demand is increasing due to growing population, climate change, and depletion of fossil fuels. This trend has given impetus to the search of efficient methods for the production of energy from renewable sources. Recent studies indicated that using solar energy to be drive for electricity and water cogeneration is both technically feasible and economically viable in geographical regions where solar irradiation is abundant and there are pressing energy and water needs [1–6]. The technologies currently under investigation are based on the concept of concentrating solar radiation to central receivers and then generating steam to power cycles and generate electricity. The most common component employed for collecting the solar radiation is mirror reflectors. The mirrored surfaces assume different shapes depending on the ultimate concentration desired. The mirrors are integrated into fixed reflectors or dishes, or sun-tracking reflectors called heliostats, which improve the concentration efficiency of the system (cf. Figure 1). The present work focuses on the latter.

The capital cost of the heliostat field in central receiver power plants is the dominant part of the system cost, reaching up to 50% of the capital investment [7]. Therefore it is essential to maximize the energy yield from a heliostat with a given mirror area. The energy yield is influenced by mirror reflectivity, blocking, and shading, as well as errors in tracking and canting methods [8]. It is difficult to experiment and rearrange the heliostat fields, so the best way to obtain performance estimates is through the use of computer simulations. Although significant amount of work is generally needed to adapt the computer codes to accommodate specific features and needs of each project, there is no consensus about which code can be considered a standard research or industry tool [9].

Garcia et al. [9] give an overview of the most widely used computer codes and detail all their features, strengths, and

Figure 1: A heliostat with square aperture.

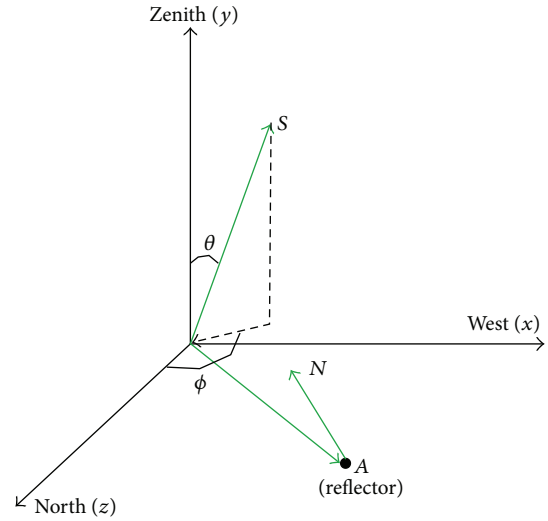

Figure 2: The global coordinate system. $\vec{S}$ is the vector to the sun, $\vec{A}$ is the vector to a point on the reflector, and $\vec{N}$ is the normal vector to the surface of the reflector.

weaknesses. These codes comprise two large categories: one category of codes utilize ray tracing to calculate concentrated solar irradiation, and another category of codes uses convolution methods. The procedure involved in ray tracing methods for specular reflection problems is to select at random a bundle of rays emitted from one surface and then track the rays that impinge on a second surface. The irradiation on an elementary surface is proportional to the number of impacting rays. This is a direct computational scheme that is essentially a Monte Carlo method. The computation time increases with the number of rays and the complexity of geometry, for a given computation accuracy.

Convolution methods take a less direct approach. Reflected rays from elementary mirrors are assigned error cones that are calculated by convolutions of normal Gaussian distributions corresponding to various error sources. These errors are a result of uncertainties in the description of reflective surfaces and sun shape properties. A systematic comparison between ray tracing and convolution methods shows that similar results can be reproduced starting from the same hypothesis [10]. Ray tracing techniques hold a great advantage over convolution methods, as they are more flexible and can be used to model nonideal optics. They can account for sophisticated physics and thus can model real interactions between the various optical components and light beams. Their disadvantage is that ray tracing codes require longer computational times, with the consequence that they are not ideal for system optimization.

Ray tracing simulation codes are based on the fundamentals of geometric optics. A *caustic* surface, or "burning" curve, in geometric optics is a boundary separating accessible and inaccessible regions for a given family of rays. The rays within that defined family can "pile up" against the boundary but they never cross it. Caustics in ray theory may be regarded as either the envelope of the rays or, equivalently, the loci of the principal centers of curvature of the wavefront. The caustic surfaces are the loci of points where the flux density is either very high or reaches a singularity. All caustics can be derived from the general integral of the eikonal equation [11].

In the present work, we utilize caustic surfaces in order to evaluate the optical performance of a single heliostat, as an alternative to the ray tracing method.

2. Methodology

The specular reflection of sun rays on a single heliostat reflector placed north of the target, both located in the north hemisphere, was examined in this work. We assume that the heliostat rotates around a point belonging to the mirror without any tracking errors. We postulate that the reflector surface can be represented by a smooth function, which is parametrized and then used to compute the caustic surfaces. The caustics are used to determine the size of the image formed on a given target, as well as the solar flux received at discreet times throughout the year.

2.1. System Geometry. We use a global coordinate system in the implementation of our model, as presented in Figure 2, which is centered on the target, with x-, y- and z-axes in the west, zenith, and north directions, respectively. The position of the sun at any instant in time can be defined by two Euler angles, the zenith angle θ and the solar azimuth angle ϕ.

From the above, it is easy to compute the global unit vector $\vec{S}$ pointing to the sun. This is given by

$$\vec{S} = \sin(\phi)\sin(\theta)\,\hat{\mathbf{i}} + \cos(\theta)\,\hat{\mathbf{j}} + \cos(\phi)\sin(\theta)\,\hat{\mathbf{k}}. \quad (1)$$

Let us choose a point A, with coordinates $\{x_A, y_A, z_A\}$, on the surface of the reflector. We require a ray from the sun that strikes this surface to be reflected to the center of the target.

In order to accomplish this the normal vector at point A must be

$$\vec{N} = \vec{S} - \frac{\vec{A}}{\left|\vec{A}\right|} = \left[\sin(\phi)\sin(\theta) - \frac{x_A}{\left|\vec{A}\right|}\right]\hat{\mathbf{i}} + \left[\sin(\theta) - \frac{y_A}{\left|\vec{A}\right|}\right]\hat{\mathbf{j}} + \left[\cos(\phi)\cos(\theta) - \frac{z_A}{\left|\vec{A}\right|}\right]\hat{\mathbf{k}}, \tag{2}$$

where $\vec{A}$ is the vector from the origin (target) to the mirror on the heliostat surface.

The surface of the reflector can be determined by employing the concept of a level surface of a smooth and nonsingular function f. The normal vector field to that level surface is such that

$$\nabla f = \vec{N}, \tag{3}$$

and solving for f, we obtain

$$f(x, y, z) = x\sin(\phi)\sin(\theta) + y\cos(\theta) + z\cos(\theta)\sin(\phi) - \sqrt{x^2 + y^2 + z^2} + A_o, \tag{4}$$

where A_0 is a constant. A family of surfaces is obtained by varying the value of the constant of integration, A_0. In order to get the surface that passes through the center of rotation of the heliostat, we set $f = 0$ and solve for A_0. Thus the surface defined by $f = 0$ will have a gradient $\vec{N}$ at each point and is the surface that focuses rays coming from the sun onto the target. By setting $f = 0$, (4) yields a conic section in three-dimensional space, known as quadric [12].

Quadrics surfaces exhibit a wide range of advantages over other families of curves. Primarily, they are second-order implicit surfaces and their behavior is well understood. Secondly, they can reproduce all ellipsoids, elliptic and hyperbolic paraboloids, hyperboloids and conic-sectioned cylinders and cones. Thus, using quadrics simplifies the design and manufacturing process used in fabricating the mirror. Moreover quadrics intersect every plane in a conic, which is particularly helpful when determining intersection points in a cutting procedure [13].

2.2. Caustic Surface. The caustic surface can be computed once the reflecting surface is defined in parametric form:

$$\vec{T}(u, v) = \left[x(u, v), y(u, v), z(u, v)\right]. \tag{5}$$

Let us suppose that the reflecting surface is illuminated by light rays. The parametric equation for a reflected ray, $\vec{R}_{\text{ref}}(s, u, v)$ propagating from point $\vec{T}(u, v)$ on the surface, can be described by

$$\vec{R}_{\text{ref}}(s, u, v) = \vec{T}(u, v) + s\vec{r}_{\text{ref}}(u, v), \tag{6}$$

where s measures distance along the reflected ray and $\vec{r}_{\text{ref}}$ is its direction of propagation which can be calculated from

$$\vec{r}_{\text{ref}}(u, v) = \vec{S} - 2\left(\vec{S}\cdot\vec{N}(u, v)\right)\vec{N}(u, v), \tag{7}$$

where $\vec{S}$ is the direction of the incoming ray and $\vec{N}(u, v)$ is the normal to the reflecting surface at the point $T(u, v)$. The locus of the caustic is determined by the points where the Jacobian of $\vec{R}_{\text{ref}}(s, u, v)$ vanishes, which produces a quadratic function in s [11].

2.3. Image on the Target. We first need to define an appropriate metric for the image size. For that we choose an appropriate length scale, such as the diameter of a circle that contains 100% of the intersected rays.

In order to determine the image formed on the target, we need to compute the intersection of the caustic with the plane of the aperture of the target. Although an arbitrary target surface can be chosen, we will simplify the problem here by considering a planar surface represented as

$$\kappa = P_0 + (P_1 - P_0)\lambda + (P_2 - P_0)\nu, \quad \kappa, \lambda, \nu \in \mathbb{R}, \tag{8}$$

where P_0, P_1, and P_2 are three points on the plane, which are not colinear. By setting the equation of the ray equal to the equation for the above plane, the points at which the reflected ray intersect the plane are obtained. The problem can be expressed in a matrix form as shown below:

$$\begin{bmatrix}\kappa\\ \lambda\\ \nu\end{bmatrix} = \begin{bmatrix}x - x_{\text{ref}} & x_1 - x_0 & x_2 - x_0\\ y - y_{\text{ref}} & y_1 - y_0 & y_2 - y_0\\ z - z_{\text{ref}} & z_1 - z_0 & z_2 - z_0\end{bmatrix}^{-1}\begin{bmatrix}x - x_0\\ y - y_0\\ z - z_0\end{bmatrix}, \tag{9}$$

where: κ, λ, ν are the coordinates of the image plane. x, y, z are the parametric equations of the reflector. x_{ref}, y_{ref}, z_{ref} are the parametric equations of the reflected ray. x_k, y_k, z_k, $k = 0, 1, 2$ are points on the plane.

3. Results

A code based on the method of caustics described above was developed in MATLAB [14]. For a given reflective surface of focal length F and aperture a, the code outputs the corresponding caustic surface, the image size, and the average flux on a planar target for a range of sun paths. The reflective surface was placed on a heliostat which is located at distance (slant range) L from the target and rotates so that the sun rays are reflected and hit the target (cf. Figure 2).

Computations were performed for location at a latitude of 34.7°, which corresponds to the coast of Pentakomo, Cyprus. To determine the angular location of the sun, the day of the year was varied from winter solstice (day 355, i.e., 21 December) to summer solstice (day 173, i.e., 21 June) following the Julian convention (i.e., 1 January being the day number 1). Computations for days outside this interval are redundant since the sun path is identical with respect to the corresponding symmetric Julian day. For instance, day 174 is identical to day 172, 175 is identical to 171, and so on. Simulations were performed for various times during the day covering the period between sunrise and sunset.

3.1. Validation. In order to validate the present algorithm, our results were compared to results we obtained from SolTRACE, a ray tracing software developed by the US

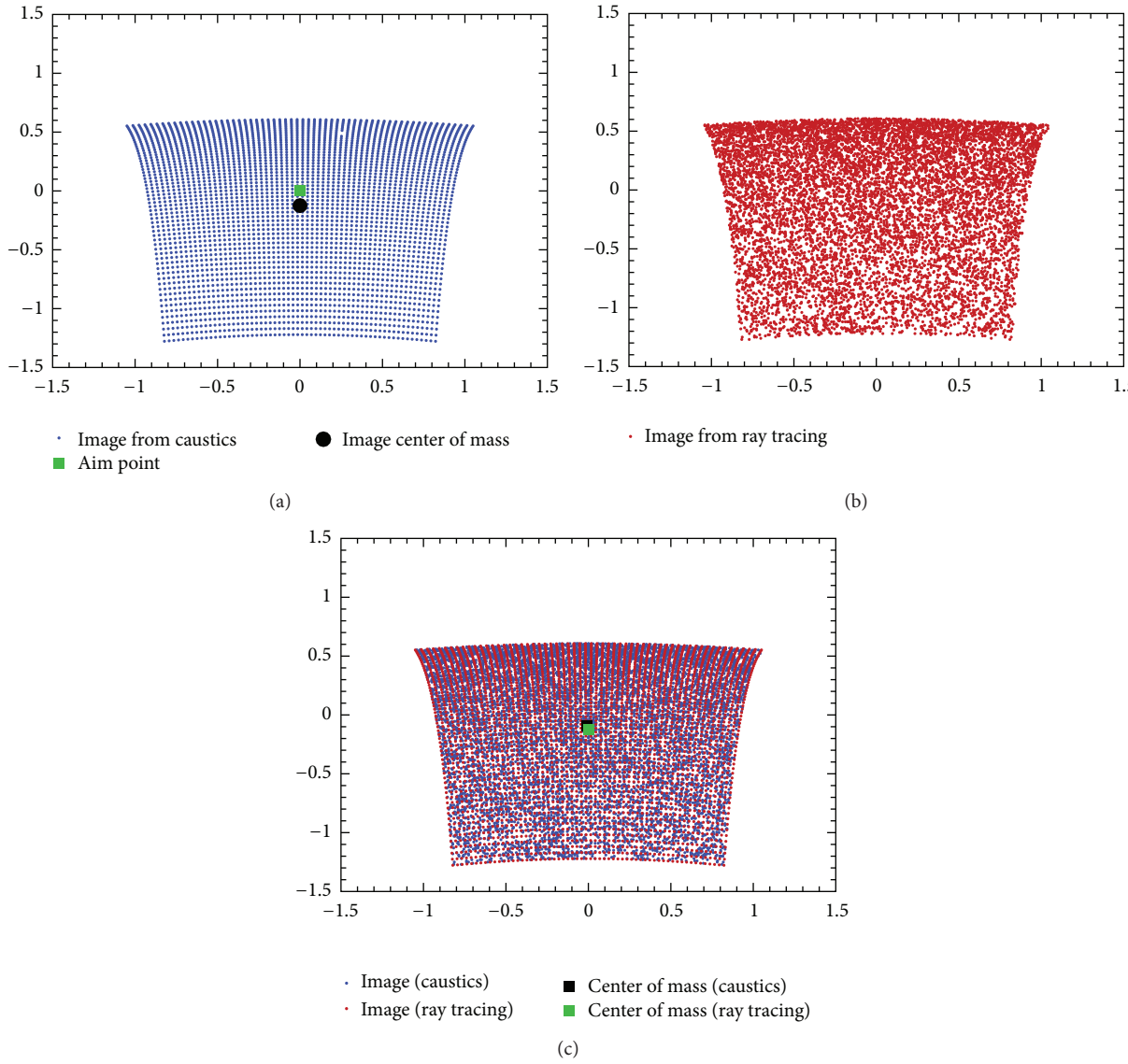

Figure 3: Image of a square parabola. (a) Image from caustics with 3600 rays. (b) Image from SolTRACE with 10000 rays. (c) Superposition of (a) and (b).

National Renewable Energy Laboratoty (NREL) [15]. This type of comparison for validation is an established practise [16]. The reflector was a paraboloid of square aperture $a = 4$ placed at $L = 25$ north. In the remaining document, dimensionless variables are used. Day and time were chosen to be day 173 and 12 noon, respectively. As is demonstrated qualitatively in Figures 3(a) and 3(b) and quantitatively in Figure 3(c), there is very good agreement between the results of the two methods. Any discrepancies are due to the fact that the number of points (i.e., ray traces on the target) in SolTRACE cannot be specified. The user can only input the number of rays that are reflected but cannot control the number that arrives at the target.

For the caustics method on the other hand a regular grid of reflection points is chosen on the mirror surface and thus results in a uniform distribution of the corresponding image points (cf. Figure 3(a)). Contrast this with the random distribution of image points from ray tracing (cf. Figure 3(b)).

3.2. Effect of Aperture to Focal Length Ratio on Solar Flux. We know from geometric optics that the focal length, F, of the reflector determines the image size and the aperture, a, determines the total energy received. Hence the ratio of aperture to focal length, a/F, determines the image brightness, or energy flux density, at the receiver of a focusing system [17]. Computations were performed to study the effect of the a/F on the flux incident on the target. A reflector with a circular aperture was tested for different aperture and focal length combinations. The reflector surface profile was a paraboloid of revolution.

Figures 4(a) and 4(b) show the average flux on the receiver aperture plane as a function of a/F for day 173. The Direct Normal Insolation (DNI) was taken to be 1000 W/m^2. As

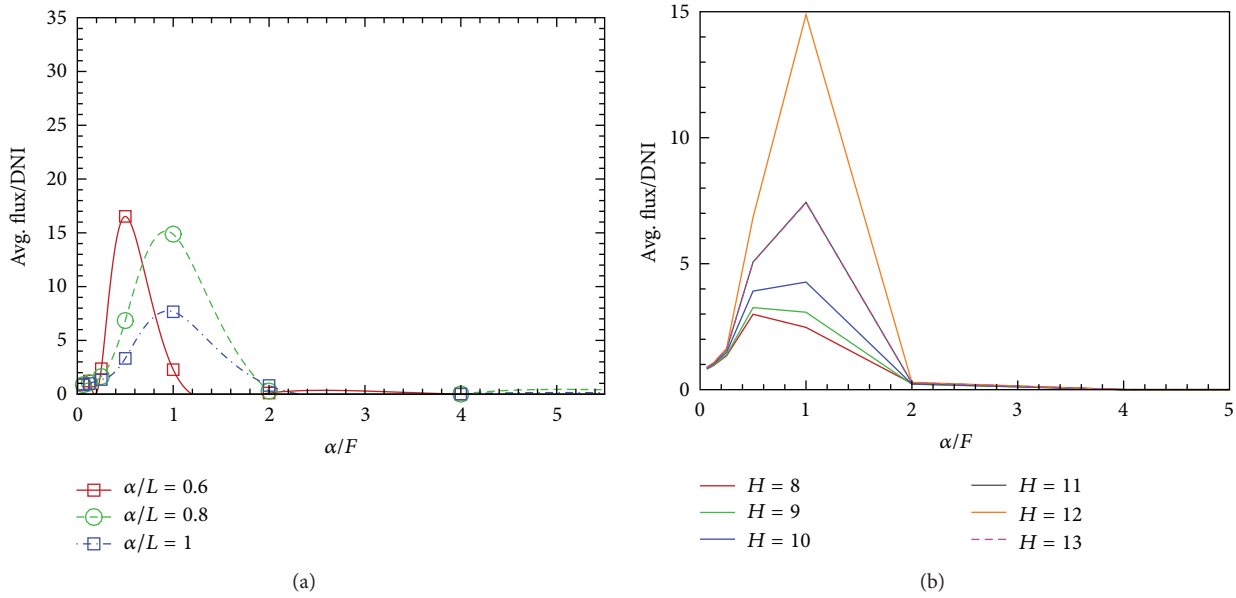

FIGURE 4: Average flux on receiver plane as a function of the aperture to focal length ratio a/F. (a) Effect of a/L on day 173 at $H = 12$. (b) Effect of time on day 173 for $a/L = 0.8$.

Figure 4 indicates, for a heliostat reflector with a given ratio of aperture to distance a/L from target, a value of a/F exists for which the flux on the target is maximum, and this optimal average flux occurs for large values of focal length (i.e., small a/F ratios). We observe that for $a/L = 0.6$, maximum average flux occurs at $a/F \approx 0.5$ and for $a/L = 0.8$, and $a/L = 1$, maximum is achieved at $a/F \approx 1$. In Figure 4(b) the hour variation of a/F is shown for day 173. We notice that the curves for $H = 11$ and $H = 13$ coincide. This is expected as the heliostat is directly north of the target so the image on the target is symmetric about noon, since the longitudinal location of the heliostat is not considered and it is assumed that solar noon is always at 12:00.

By performing additional calculations for other days during the year, we found that the value of a/F, for which maximum flux on the receiver is achieved, does not exhibit a yearly or hourly variation. Thus by utilizing the two ratios a rapid and fairly uncomplicated method of optimizing the entire heliostat field is developed.

3.3. Sun Image Size from Reflectors Modeled by Simple Quadric. Since the reflector surface constitutes the most costly component of the solar collection system, it is better to consider simple shapes, which can easily be fabricated. We are studying here the performance of reflectors modeled by conic sections for various a/F ratios.

3.3.1. Paraboloid of Revolution. The most common reflector profile in solar thermal applications is paraboloid. Let us start by considering the following equation for a quadric surface with a focal point at the origin:

$$P(x, y, z) = \frac{y^2}{b^2} + z^2 + 4F(x - F) = 0, \tag{10}$$

which can be parametrized via u and v as follows:

$$\vec{G}(u, v) = \begin{bmatrix} x(u, v) \\ y(u, v) \\ z(u, v) \end{bmatrix} = \begin{bmatrix} F\left(1 - u^2\right) \\ 2Fb_y u \sin(v) \\ 2Fb_z u \cos(v) \end{bmatrix}, \tag{11}$$

where $-\infty < u < +\infty$ and $-\pi/2 < v < \pi/2$. In the above equation, b_y, b_z are equivalent of the stretching factor introduced in [8] in both the lateral and vertical directions of the mirror, in order to allow further adjustment of the individual facet mirrors.

By setting $b_y = b_z = 1$, (11) reduces to the equation of a paraboloid of revolution. We consider here a paraboloid of revolution mirror of aperture $a = 10$, with a focal point at $L = 25$. The caustic for an incident angle of $\omega = \pi/5$ is presented in Figure 5(a). As mentioned in Section 2.2, the locus of the caustic is where the Jacobian of $\vec{R}_{\text{ref}}(s, u, v)$ vanishes. Since the Jacobian is quadratic in s, the caustic has a positive and negative branch. The intersection of the caustic with the target was estimated and depicted in Figure 5(b).

The effect that the variation of the a/F ratio has on the image size was examined using caustics. As Figure 6 indicates, there is a value of a/F for which the image size is minimum. We define as image size the distance between the weighted center of mass of all the points and the farthest point on the boundary, for example, D_{100}.

4. Discussion

Caustic surfaces were employed in order to compute the solar image size and flux density on a stationary and predefined target corresponding to the receiver. The mathematical analysis of Section 2 indicates that the reflector surface should be a quadric, which is the manifestation of a conic section in

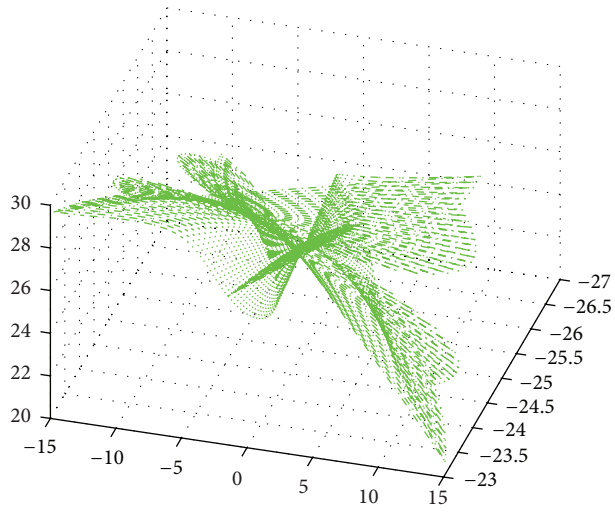

(a) The positive and negative branches of the caustic

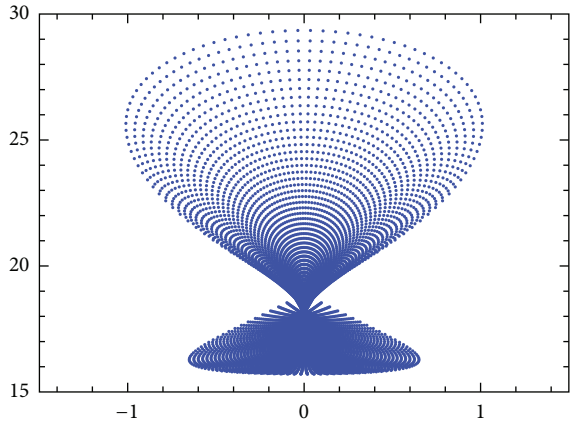

(b) Image at the target when $\omega = \pi/5$

FIGURE 5: Results for Paraboloid of revolution when $\omega = \pi/5$.

three-dimensional space. The algorithm for the construction of caustics was validated for a reflector described by a paraboloid of revolution with a square aperture by comparing the results to those obtained by SolTRACE. An excellent agreement in image size was obtained between the two codes. The only discrepancy is the difference in imaging ray density since we cannot predefine the distribution of rays on the target in SolTRACE, while we used a uniform grid in the caustics computation.

In order to gain some insight the caustic surface of a paraboloid reflector was computed and the image on the target was reconstructed using our numerical code. The effect of varying the aperture to focal length ratio a/F and the aperture to slant length ratio a/L on the image size and flux was also investigated. Both ratios affect the energy flux concentration on the target of the focusing system. We demonstrated that there is an a/F ratio which maximizes the average flux on the target, and it increases with a/L. It was also shown that the value of a/F, for which maximum flux on the receiver is achieved, does not exhibit a yearly or hourly variation.

We have established a methodology whereby, given a characteristic dimension of the aperture of a reflector, the

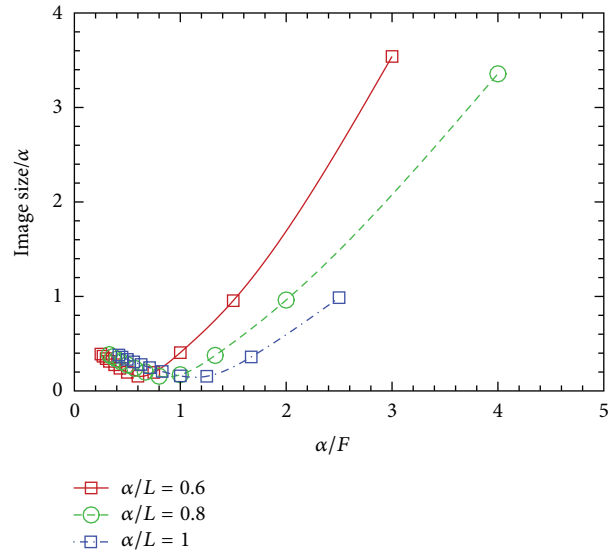

FIGURE 6: Effect of varying a/F ratio on image size of sun reflected on a paraboloid of revolution.

optimal focal length is determined such that maximum flux is delivered to the target and the spillage is minimized. Thus, in principle and for a large solar collector field, one should use reflectors of different sizes and shapes to maximize the solar energy capture. This choice should of course be weighted against the economic advantage gained by mass-producing identical mirrors for the heliostats. There are also proposals, involving heliostats with adaptive surfaces (i.e., consisting of mirror segments that are actuated and move independently). In such designs, there are advantages in maximizing flux and limit spillage for each heliostat through the field.

The main motivation of this work was to examine the applicability and advantages of caustics in simulating components for concentrated solar power applications. In codes that utilize ray tracing methodology to compute the image, the user selects a given number of rays to be traced. Each ray traced through the possible optical paths corresponds to a random step of a Monte Carlo method. Image accuracy increases in the number of rays traced but larger ray numbers mean more processing time. Consequently, complex geometries translate into longer run times. Caustics can be constructed analytically as opposed to the stochastic techniques at the heart of an off-the-shelf ray tracing software.

Methodologies using caustics are in principle much faster than ray tracing because they involve the construction of a mathematical surface coupled to the geometry of the reflector surface. Hence, accuracy does not depend on the number of points but on the accuracy of the reflector surface description. Of course the computational time required for caustics in Figure 3(a) increases as the geometry increases in complexity, since the Jacobian matrix of the reflected ray needs to be computed for every combination of sun position and heliostat. Nevertheless, the advantage of using caustics for concentrated solar power calculations lies with the construction of the outline of the solar image on the target, which determines the amount of spillage. It is computationally more efficient to find

the intersection of two surfaces (i.e., caustics and target) than to reconstruct it from the iterative ray tracing computation occurring in three dimensions.

Finally there is another advantage in the caustics formulation which has not been explored in this work. All the monochromatic aberrations associated with a wavefront train and ultimately with the object that generates it are included in the caustic. The structure of this caustic contains the effects of the image errors, such as spherical aberration, coma, and astigmatism, as its location in space accounts for the field errors such as distortion and field curvature [18]. This is a very convenient feature because after the caustic is constructed, no further derivations are necessary to take these errors into consideration. Since the caustic contains all the required information to compute the image size one can quickly determine the image size of each receiver geometry without having to generate random rays on the reflector as is the case for ray tracing methods. Although a planar target receiver was considered here, a curved receiver surface can easily be conceptualized so it conforms to year.

5. Conclusions

There is no question that renewable energy, in particular solar energy, has an important role to play in meeting our future energy requirements. The use of concentrated solar power, to drive a single or dual purpose plant, is an emerging technology whose efficient implementation requires the proper scaling of the optical and the thermal components.

Heliostat mirror remains one of the key optical components in solar energy concentration applications. This study was motivated by the need to develop a computer code in order to simulate, model, and compute the image size and flux on a target from solar light reflected from a mirror mounted on a heliostat. The accurate determination of image size and flux is of great significance, since minimizing the image size means higher concentration ratios, which imply higher solar receiver temperatures and higher power cycle efficiencies.

We demonstrated that caustic surfaces are viable alternative to ray tracing. These surfaces form the boundary between inaccessible and accessible areas for a given family of reflected rays and are characterized as the loci of points where energy flux is maximum. The construction of the caustic involves the determination of a geometric object which contains all possible image errors. It is thus computationally more efficient to use caustics to determine the intersection of the reflected beam with the target as a function of both the reflector and target characteristics than rely on a Monte Carlo technique.

Acknowledgments

This work is a product of an interdisciplinary collaboration between the Cyprus Institute and the University of Illinois at Urbana-Champaign. We gratefully acknowledge the funding from the Cyprus Research Promotion Foundation for the CyI and the USA National Science Foundation under Water-CAMPWS Science and Technology Center (CTS-0120978) and EAGER Grant (CBET-0941254) for UIUC.

References

[1] F. Trieb, "Concentrating solar power for seawater desalination," Tech. Rep., German Aerospace Center (DLR), Stuttgart, Germany, 2007.

[2] C. Papanicolas, "Research and development study for a concentrated solar power-desalination of sea water (CSP-DSW) project," Tech. Rep., The Cyprus Institute, Nicosia, Cyprus, 2010.

[3] A. Ghobeity, C. Noone, C. Papanicolas, and A. Mitsos, "Optimal time-invariant operation of a power and water cogeneration solar-thermal plant," *Solar Energy*, vol. 85, no. 9, pp. 2295–2320, 2011.

[4] A. Vozar-McKnight, M. Georgiou, M. Seong, and J. Georgiadis, "Analysis and design of a multi-effect desalination system with thermal vapor compression and harvested heat addition," *Desalination and Water Treatment*, vol. 31, no. 1–3, pp. 339–346, 2011.

[5] M. J. Montes, A. Rovira, M. Muñoz, and J. M. Martínez-Val, "Performance analysis of an integrated solar combined cycle using direct steam generation in parabolic trough collectors," *Applied Energy*, vol. 88, no. 9, pp. 3228–3238, 2011.

[6] S. Janjai, J. Laksanaboonsong, and T. Seesaard, "Potential application of concentrating solar power systems for the generation of electricity in Thailand," *Applied Energy*, vol. 88, no. 12, pp. 4960–4967, 2011.

[7] G. Kolb, S. Jones, M. Donnelly et al., "Heliostat cost reduction study," Tech. Rep. SAND2007-3293, Sandia National Laboratories, Albuquerque, New Mexico, 2007.

[8] R. Buck and E. Teufel, "Comparison and optimization of heliostat canting methods," *Journal of Solar Energy Engineering*, vol. 131, no. 1, Article ID 011001, 8 pages, 2009.

[9] P. Garcia, A. Ferriere, and J. J. Bezian, "Codes for solar flux calculation dedicated to central receiver system applications: a comparative review," *Solar Energy*, vol. 82, no. 3, pp. 189–197, 2008.

[10] R. Pitz-Paal and P. Schwarzbozl, "Software developments for system analysis and optimization," SolarPACES, 2000.

[11] C. G. Bell, H. Ockendon, and J. R. Ockendon, "The caustics of two- and three-dimensional parabolic reflectors," *Journal of Optics*, vol. 12, no. 6, Article ID 065703, 2010.

[12] N. Gonçalves, "On the reflection point where light reflects to a known destination on quadratic surfaces," *Optics Letters*, vol. 35, no. 2, pp. 100–102, 2010.

[13] J. Fan and A. Ball, "Quadric method for cutter orientation in five-axis sculptured surface machining," *International Journal of Machine Tools and Manufacture*, vol. 48, no. 7-8, pp. 788–801, 2008.

[14] MathWorks, "Matlab," 2009.

[15] T. Wendelin, "Soltrace: a new optical modeling tool for concentrating solar optics," in *Proceedings of the International Solar Energy Conference (ISEC '03)*, ASME Conference Proceedings, no. 36762, pp. 253–260, March 2003.

[16] C. J. Noone, M. Torrilhon, and A. Mitsos, "Heliostat field optimization: a new computationally efficient model and biomimetic layout," *Solar Energy*, vol. 86, no. 2, pp. 792–803, 2012.

[17] J. Duffie and W. Beckman, *Solar Engineering of Thermal Processes*, Wiley, 3rd edition, 2006.

[18] O. Stavroudis, *The Mathematics of Geometrical and Physical Optics*, Wiley-VCH, GmbH & Co. KGaA, 2006.